Journal of The Electrochemical Society, **159** (11) H823-H827 (2012)
0013-4651/2012/159(11)/H823/5/$28.00 © The Electrochemical Society

Antibacterial Activity and Photocatalysis of Electrosprayed Titania Films

Hyun Yoon, Bhavana Joshi, Seung-Heon Na, and Sam S. Yoon[z]

School of Mechanical Engineering, Korea University, Seoul 136-713, Korea

Titanium dioxide (TiO_2) films were successfully deposited on conductive glass substrates by electrostatic spray. The effect of annealing temperature on the structural and photocatalytic properties of TiO_2 films were studied by X-ray diffraction, scanning electron microscopy, AFM (Atomic Force Microscopy), and UV visible spectroscopy. TiO_2 films annealed at higher temperatures showed excellent photocatalytic activity through degradation of methylene blue under UV irradiation. The highest photocatalytic activity (92.2% photodegradation of methylene blue after 4 hours irradiation under UV light) was measured for a TiO_2 film annealed at 500°C because of the formation of a nanocrystalline anatase phase. The antibacterial capabilities of annealed TiO_2 were measured against gram-negative bacteria (*Escherichia coli*) under UV light ($\lambda = 365$ nm and $I = 0.6$ mW/cm^2) and in the dark. Complete sterilization was observed with TiO_2 films annealed at 500°C and 600°C after 1 hour of UV illumination
 [DOI: 10.1149/2.002211jes]

Manuscript submitted June 11, 2012; revised manuscript received July 23, 2012. Published August 31, 2012.

Titanium dioxide (TiO_2, anatase) is a semiconductor material having a bandgap value of 3.2 eV.[1] Research on the photocatalytic activity of TiO_2 has been extensively reported since water was split by TiO_2 under ultraviolet (UV) light by Fujishima and Honda in 1972.[2] TiO_2 is abundant in nature, non-toxic, biocompatible, has low cost, strongly oxidative, manufacturable at atmospheric conditions, and environmentally friendly. Thus, TiO_2 is used in many products for self-cleaning applications,[3] bactericidal treatment,[4–10] dye-sensitized solar cells,[11] etc. In air and water purification,[12–14] the photocatalytic effect of TiO_2 is used for odor removal, decoloring wastewater,[15] mineralization of both hazardous organic and inorganic materials,[16] and soil decontamination.[17] Biocompatibility of TiO_2 makes it useful for implants, drug delivery systems, cell growth, biosensors, immunoisolations, bioartificial organs, and tissue engineering.[18]

When TiO_2 is irradiated with near UV light ($\lambda < 388$ nm),[19] charge separation occurs when an electron is excited from valence band to conduction band, leaving a hole in the valance band. These photogenerated electrons in TiO_2 react with atmospheric oxygen to yield superoxide radical anions ($^{\bullet}O_2^-$), while the holes, in the valance band react with ambient water to form hydroxyl radicals ($^{\bullet}OH$) and hydrogen peroxide (H_2O_2). These highly oxidizing hydroxyl radicals are useful for killing bacteria or degrading toxic compounds in water or air.

Photocatalysis is an interfacial phenomenon,[20] hence nanostructured TiO_2 surfaces exhibit superior photocatalytic activity due to a high surface area-to-volume ratio, thereby enhancing efficient UV irradiance with high quantum yields.[21] There are common ways of disinfecting fluids with TiO_2. The first is a *mobilized* mode; TiO_2 powders in an aqueous medium to efficiently degrade contaminants due to the high surface area.[22] However, this mobilized mode requires a costly solid-liquid separation post-process like sedimentation, centrifugation, or coagulation, which is difficult and time consuming. There is also an *immobilized* mode whereby a thin film is coated on substrates like quartz, a fiber mat, a mesh, or stainless steel. The fluid is then brought into contact with the immobilized TiO_2 for disinfection.

Various vacuum techniques have been used to deposit TiO_2 films such as reactive magnetron sputtering,[23] electron beam evaporation,[24] metal organic chemical vapor deposition,[25] chemical vapor deposition,[26] and pulsed laser deposition.[27] Non-vacuum techniques include sol-gel,[28–30] doctor blading,[31] screen printing,[32] flame aerosol reactor systems,[11] aerosol deposition,[33] and electrostatic spray deposition (ESD).[34,35] A schematic illustrating an antibacterial film fabricated by the ESD (Electrostatic Spray Deposition) system is shown in Figure 1. Among these various deposition systems, ESD is attractive because it produces extremely fine (sub-micron), self-dispersive (non-agglomerating), highly wettable (electrowetting), adhesive droplets that yield a uniform coating on the substrate. Electrospraying can produce pure materials with structural control at the nanometer scale. The crystallinity, surface texture, film thickness, and deposition rate can be easily controlled by adjusting voltage, flow rate, precursor concentration, and the substrate temperature. In addition, because charged droplets are accelerated toward the substrate, ESD offers improved targeting, which results in high deposition efficiency and low material consumption.[36]

This paper studies the characteristics of nano-crystalline TiO_2 films manufactured by an ESD technique for antibacterial applications. TiO_2 films with thickness >1 μm are important because they absorb UVA (320 to 380 nm) light, which comprises 99% UV light reaching the earth from sun.[37] To the best of our knowledge, we are the first to study the antibacterial properties of ESD-coated TiO_2 films. Post-annealing increases the anatase phase and induces changes to the film's surface roughness and density. The effect of annealing temperature on TiO_2 decolorization of methylene blue (MB) and the number of surviving bacterial colonies under UV illumination are investigated. MB was selected as a model organic pollutant.

For the antibacterial study, *E. Coli* gram-negative bacteria was selected because it is considered an indicator of fecal contamination and is widely used as a model microorganism for physiological, biochemical, and antibacterial tests of different chemical substances and materials. In addition, it causes urinary tract infections, sepsis/meningitis, and enteric/diarrheal disease.

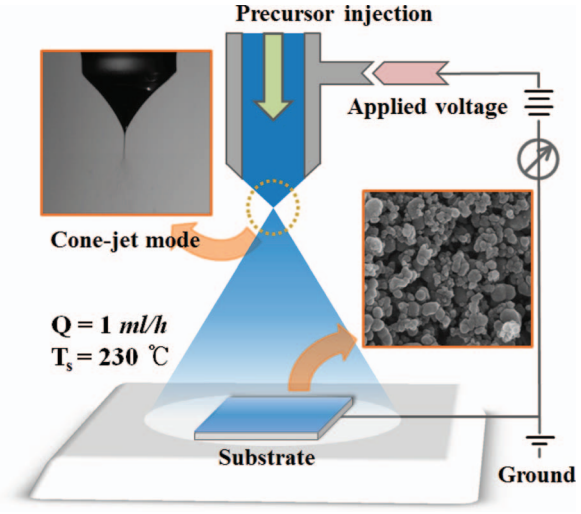

Figure 1. Schematic illustrating an antibacterial film fabricated by the ESD (Electrostatic Spray Deposition) system. Q is flowrate and T_s is substrate temperature.

[z]E-mail: skyoon@korea.ac.kr

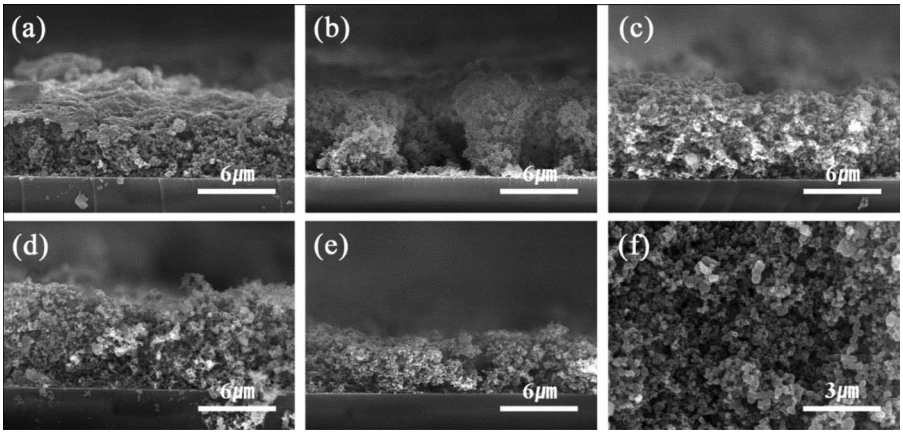

Figure 2. SEM cross-sectional view of TiO_2 films (a) as-deposited (b) 300, (c) 400, (d) 500, and (e) 600°C plus (f) the surface morphology of the film annealed at 500°C.

Experimental

Preparation of the thin films.— ESD of thin TiO_2 films started with titanium tetraisopropoxide (TTIP, $Ti[OCH(CH_3)_2]_4$, 97%, *Sigma-Aldrich*) as the precursor in liquid form. The spray solution is prepared as a mixture of TTIP with deionized water, ethyl alcohol (C_2H_5OH, 99.9%, *Duksan* chemical) and DEG ($C_4H_{10}O_3$, *Duksan* chemical) in volume ratio of 1:1.5:50:50. The solution was stirred at room temperature. Next, ethanol evaporated by heating the solution to 80°C. This ethanol-free precursor was used to form a stable Taylor cone for ESD. Indium tin oxide (ITO) -coated glass was used as the conductive substrate. However, it is important to note that the ITO layer stops migration of sodium and other foreign atoms from the glass substrate that may reduce the photocatalytic activity of deposited films.[38] Prior to deposition of the TiO_2 film, the ITO-coated glass substrates were first cleaned in an ultrasonic ethanol bath and dried. The precursor solution is electrostatically sprayed using a 1-mL/hour flowrate onto the pre-heated ITO substrate at 230°C for film pyrolysis. A deposition time of 20 minute (min) was used to deposit all TiO_2 thin films. Finally, the films were annealed in a closed furnace for 10 min at temperatures ranging from 300 to 600°C.

Characterization of the thin films.— The crystalline structures of the as-deposited and annealed TiO_2 films were determined by X-ray diffraction (XRD, *Rigaku*, D/max-2500) with Cu kα ($\lambda = 0.154$ nm). Surface morphologies and cross sectional views of the films were imaged with a scanning electron microscope (HRSEM, *Philips*, L30SFEG at 10 kV). A non-contact mode atomic force microscope (AFM *Park Systems* Xe-100) was used to examine the surface morphology and roughness of the electrosprayed films.

Photocatalytic degradation of MB.— The photocatalytic effect of TiO_2 films was studied through photodegradation of an aqueous MB solution (3×10^{-2} M). The aqueous MB solution was poured evenly onto the TiO_2 films annealed at different temperatures and irradiated under UV light ($\lambda = 365$ nm and $I = 0.6$ mW/cm^2). Next, the MB solution was collected after 1 hour and changes in concentration were estimated by measuring the intensity of the MB absorption peak at 664 nm using the UV–visible spectrometer (Optizen POP Mecasys Co. LTD, Korea).[39] Similarly, the effect of irradiation time on MB degradation was also investigated. Tests were repeated to confirm the reliability of the results.

Photocatalytic inactivation of E-Coli bacteria:.— The antibacterial activity of annealed TiO_2 films under UV illumination was measured using *E. coli* bacteria. *E. coli* colonies were incubated in a nutrient broth at 37°C for 24 hour before the antibacterial test. These activated bacteria suspensions were centrifuged at 300 rpm for 10 min and bacterial cells were collected. These bacteria were mixed with a phosphate buffered saline (PBS) solution to a concentration of bacterial cell $\sim 2 \times 10^6$ colony-forming units per milliliter (CFU/mL). About 100 μL of the final *E. coli* solution was dropped on the annealed TiO_2 films in a petri dish and irradiated under the UV light for 1 hour. After 1 hour, the bacteria were washed and collected from the surface of the film using 100 mL of PBS solution. About 100 μL of this bacteria/PBS solution was placed on nutrient agar plates. The number of surviving bacterial colonies on the agar plate was counted after incubation for 24 hour at 37°C. Average counts across three plates for each film were reported.

Results and Discussion

Figure 2a-2e are cross-sectional views from the SEM of the as-deposited and annealed TiO_2 films. Film thickness decreased from 7 to 5 μm with increasing annealing temperature from 300 to 600°C. The surface morphology of TiO_2 film annealed at 500°C is highly porous as shown in Figure 2f. The SEM surface profiles of films annealed at 300 and 400°C films are similar, whereas the film annealed at 600°C is denser than the film annealed at 500°C (it is the thinnest for the same amount of TiO_2 deposited).

The surface roughness of as deposited and annealed TiO_2 thin films was measured with the AFM. Top- (2D) and angle- (3D) view images in Figure 3 illustrate the surface morphologies of a

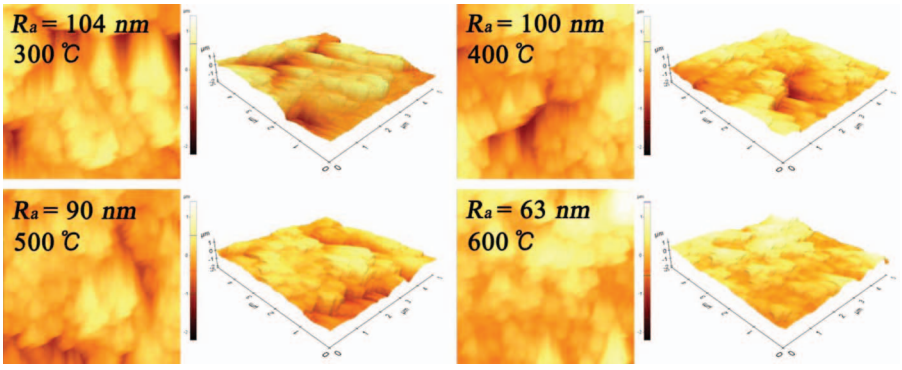

Figure 3. Top-(2D) and angle-(3D) view AFM images of the films annealed at temperatures from 300 to 600°C. Note, that R_a is the surface roughness.

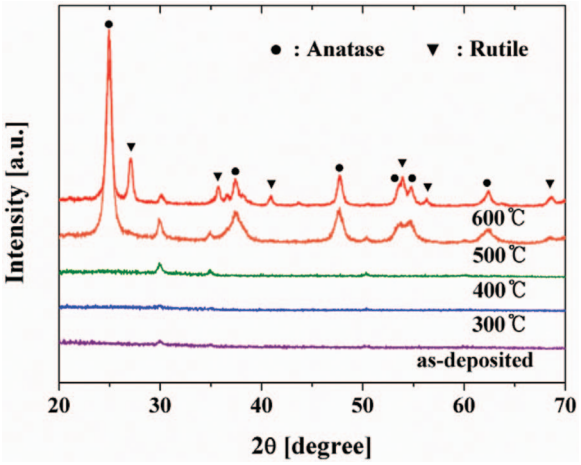

Figure 4. XRD spectra of as-deposited and various temperatures annealed TiO_2 films.

$5 \times 5\text{-}\mu m^2$ area of the annealed TiO_2 films. The films annealed at 300 and 400°C have more surface roughness (R_a) due to the presence of an amorphous phase and higher porosity. However, as the annealing temperature increased from 500 to 600°C, the surface roughness notably decreased due to increased crystal size (as observed by XRD).[40] The 2D AFM images of 300, 400, and 500°C annealed samples indicate some surface porosity (dark regions). The film annealed at 600°C is least porous with fewest dark regions (densest), in agreement with the SEM cross-section view of Figure 2e.

The X-ray diffraction patterns of the as deposited and annealed TiO_2 films are shown in Figure 4. The presence of a polycrystalline TiO_2 thin film at higher annealing temperatures is confirmed by the XRD spectra. The as-deposited and lower-temperature annealed films (up to 400°C) show the featureless pattern of an amorphous state. With an increase in annealing temperature up to 500°C, the amorphous phase is crystallized into an anatase phase confirmed by peaks at $2\theta = 25.06$, 37.53, 47.82, 53.66, 54.86, and 62.34° corresponding to the (101), (001), (200), (105), (211), and (204) orientation planes, respectively, that are in agreement with JCPDS card 21-1272. The peaks in the TiO_2 film annealed at 600°C also show sharp anatase signatures at the aforementioned diffraction angles plus additional peaks from the rutile phase at $2\theta = 27.14$, 35.80, 38.37, and 54.08° corresponding to the (110), (101), (200), and (211) orientation planes, respectively. The rutile peaks are also in agreement with JCPDS card 21-1276. The transformation temperature from amorphous to anatase phase is between 400 and 500°C, which is also true for TiO_2 films made with other techniques.[41] The average TiO_2 crystallite size of the anatase phase determined from the XRD patterns with the Scherrer equation increase from 13.28 to 16.16 nm for films annealed at 500 and 600°C, respectively.[35] The relative weight fractions of the anatase (W_A) and rutile (W_R) phases are calculated using the relationship $W_A = 1/(1 + 1.265 I_R/I_A)$ and $W_R = 1/(1 + 0.8 I_A/I_R)$ where I_A and I_R are the intensity of peaks at 25.06° (anatase) and 27.14° (rutile) respectively.[42] For the TiO_2 film annealed at 600°C, this yields a mixture of 79.6% anatase and 20.4% rutile phases.

To understand the role of TiO_2 surface structure, the effect of annealing temperature on the photocatalytic activity of films was evaluated after UV illumination by measuring the decomposition of an aqueous MB solution. The reaction mechanism of MB degradation in presence of TiO_2 under UV irradiation is:

$$TiO_2 + h\nu\,(UVA) \rightarrow TiO_2\left(h^+_{vb}\right) + TiO_2(e^-_{cb})\,(Generation\ of\ electron\ hole\ pair) \quad [1]$$

$$TiO_2\left(h^+_{vb}\right) + H_2O \rightarrow H^+ + TiO_2(\cdot OH\,(OH\ radical\ formation) \quad [2]$$

$$TiO_2(e^-_{cb}) + O_2 \rightarrow TiO_2\,(O_2^{-\cdot})\,(Superoxide\ anion\ radical) \quad [3]$$

The photocatalytic activity of TiO_2 starts with irradiation by UV light ($\lambda = 365$ nm) that generates the electron hole pairs. In the presence of oxygen, electron scavenging yields superoxide radicals ($O_2^{-\cdot}$) while the holes react with water to form a hydroxyl radical (OH). Recombination of hole electrons is prevented upon formation of surperoxide and hydroxyl radicals

$$TiO_2\,(O_2^{-\cdot}) + H^+ \rightarrow HO_2 \quad [4]$$

$$2HO_2 \rightarrow H_2O_2 + O_2\,(H_2O_2\ generation) \quad [5]$$

$$H_2O_2 + TiO_2\,(e^-_{cb}) \rightarrow TiO_2\,(\cdot OH) + OH^-\,(More\ OH\ radical\ formation) \quad [6]$$

$$TiO_2\,(\cdot OH) + MB \rightarrow \text{degradation products} + TiO_2 \quad [7]$$

$$TiO_2\,(O_2^{-\cdot}) + MB \rightarrow \text{degradation products} + TiO_2 \quad [8]$$

Hydroxyl and superoxide radicals react with MB (reaction steps 7 and 8) to yield degradation products like CO_2, NO_3, NH_4^+, SO_4^{-2}

$$MB + TiO_2 \xrightarrow{(h\nu UVA)} CO_2 + H_2O + NO_3 + NH_4^+ + SO_4^{-2} + TiO_2 \quad [9]$$

Figure 5 shows the decrease in MB concentration with increasing irradiation time for TiO_2 films annealed at 500°C. The decrease in MB absorbance peak after 4 hours of UV irradiation indicates a 93% degradation of MB solution due to the photocatalytic activity of anatase-TiO_2. The inset photograph in Figure 5 represents the decolorization of MB solution with increasing irradiation time.

The degradation of MB solution after 1 hour of UV irradiation in presence of TiO_2 films annealed at temperatures ranging from 300 to 600°C is presented in Figure 6. The MB degradation is measured through changes in absorbance of 664 nm UV light. The concentration of MB was calculated from an absorbance vs. concentration calibration curve to evaluate the degradation efficiency.[43] Amorphous TiO_2 films (annealed at 300 and 400°C) showed only 51 to 56% photocatalytic activity, which can be correlated to structural imperfections such as porosities within the amorphous structure. These imperfections generate additional electronic states that increase the recombination rate of electron holes and lower the production of OH radical resulting in reduced photocatalytic activity. The greatest degradation of MB was observed for TiO_2 films annealed at 500°C after UV irradiation. Table I shows that degradation efficiency increases with

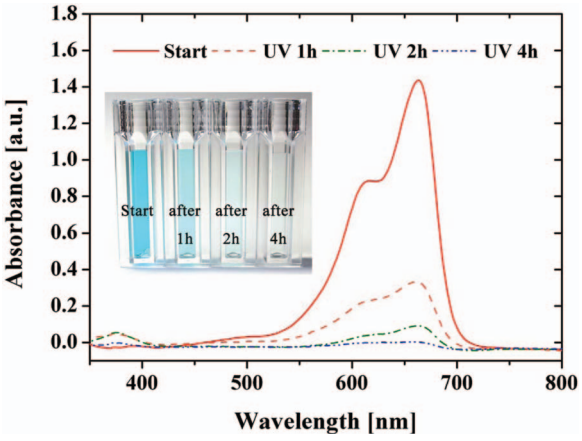

Figure 5. UV-visible spectra of aqueous MB solution in the presence of a TiO_2 film annealed at 500°C as function of UV illumination time. Inset shows decolorization of MB.

Table I. Annealing temperature effect on degradation efficiency after 1 hour of UV irradiation.

Temperature (°C)	300	400	500	600
Degradation efficiency (%)	51.1	56.3	70.2	65.6

Table II. Effect of UV irradiation time on MB in the presence of a TiO_2 film annealed at 500°C.

Time (hour)	1	2	4
Degradation efficiency (%)	70.2	87.4	92.90

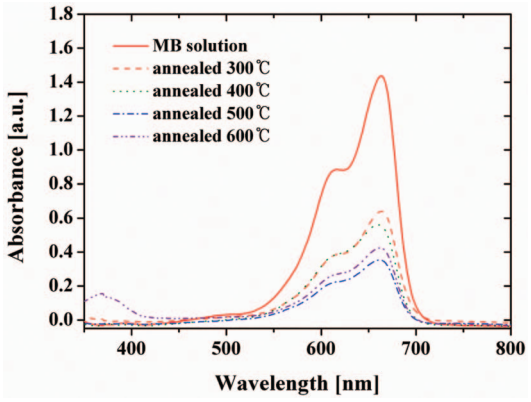

Figure 6. UV-visible spectra of aqueous MB solution as a function of annealing temperature for TiO_2 films illuminated with UV for 1 hour.

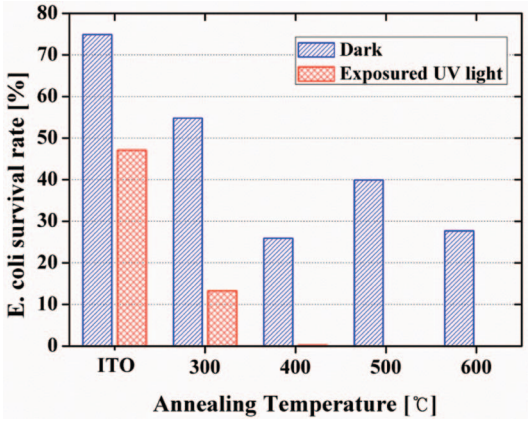

Figure 7. Survival rate of *E. Coli* bacteria in the dark and under UV irradiation in contact with annealed TiO_2 films.

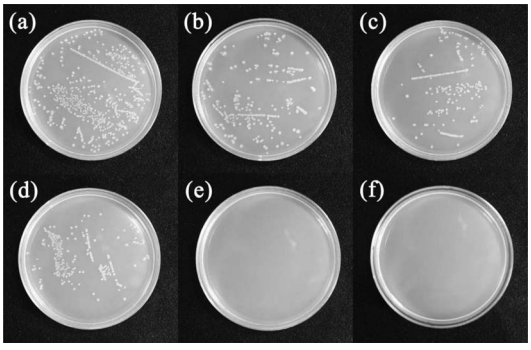

Figure 8. The top row, (a)-(c), shows bacteria colonies under dark conditions in the presence of (a) the ITO substrate and annealed TiO_2 films at (b) 500 and (c) 600°C. The bottom row, (d)-(f), demonstrates antibacterial effects after 1 hour of UV irradiation for (d) the ITO substrate and annealed TiO_2 films at (e) 500 and (f) 600°C.

increasing annealing temperature (except 600°C), which we ascribe to the crystalline transformation of TiO_2 films from an amorphous to an anatase phase. In general, the photocatalytic activity of anatase is higher than amorphous and rutile TiO_2. The film annealed at 600°C shows increased degradation efficiency compared to films annealed at 300 and 400°C due to the presence of 79.6% anatase phase. Table II shows how degradation efficiency changes with time; it increases for longer UV exposure.

Reduction of bacteria is categorized into four groups. 1–20% reduction in bacteria means no antibacterial activity, 20–50% reduction indicates low antibacterial effect, between 50–70% reduction suggests a significant antibacterial effect and >70% reduction is considered a powerfully antibacterial.[44] A quantitative evaluation of antibacterial activity of annealed TiO_2 films was carried out. Figure 7 shows the survival rate of *E coli* under UV light illumination and in the dark.[45] The ITO substrate after 1 hour of UV irradiation has a 47% survival ratio. The antibacterial activity in this case is due to the UV light itself.[46] Srinivasan et al.[47] reported that, even if the survival rate of bacteria is less without TiO_2 the concentration of endotoxin increases due to killing of bacterial cells. However, when a TiO_2 film is used as a photocatalyst, the outer membrane of the *E. coli* cell is destroyed and endotoxin is degraded. The survival rates of bacteria after 1 hour of UV irradiation for TiO_2 films annealed at 300 and 400°C are 13 and 0.2%, respectively. Under the same conditions all bacteria were killed by films annealed at 500 and 600°C. The antibacterial activity increases with increasing annealing temperature due to transformation of TiO_2 from an amorphous to an anatase phase. The snapshot in Figure 8a shows essentially no antibacterial effect. There is a low antibacterial effect (Figure 8d) after UV irradiation for 1 hour. Figure 8b, 8c shows significant antibacterial effects. Complete sterilization was observed for UV-exposed TiO_2 films annealed at 500 and 600°C (Figure 8e, 8f). This qualitatively demonstrates the antibacterial efficacy of TiO_2, which generates reactive radicals that penetrate bacteria cell walls ultimately leading to their death.

Conclusions

TiO_2 films were deposited by ESD and the effects of annealing temperature on photocatalysis and antibacterial properties were studied. XRD peaks confirmed the presence of a polycrystalline anatase phase with a crystallite size of 13.28 nm at a 500°C annealing temperature. Increasing the annealing temperature to 600°C yields an anatase/rutile mixed phase TiO_2 film with a dense surface morphology. Excellent photocatalytic activity was observed for TiO_2 film annealed at 500°C with 93% decomposition of MB after UV irradiation for 4 hours. These polycrystalline TiO_2 films exhibit antibacterial properties against *E. coli*, but films annealed at 500 and 600°C shows complete sterilization.

Acknowledgments

This work was supported by the Human Resources Development of the Korea Institute of Energy Technology Evaluation and Planning (KETEP, No. 20104010100640), National Research Foundation of Korea (NRF-2012-0001169), and the Converging Research Center Program through the Ministry of Education, Science and Technology (2010K000969). This work was also supported by the National Research Foundation of Korea (NRF-2011-0030433 and 2010-0010217) grant funded by the Korean government (MEST) and by a grant from the cooperative R&D Program (B551179-08-03-00) funded by the Korea Research Council Industrial Science and Technology.

References

1. C. M. Teh and A. R. Mohamed, *J. Alloys Compd.*, **509**, 1648 (2011).
2. A. Fujishima and K. Honda, *Nature*, **238**, 37 (1972).
3. K. Guan, *Surf. Coat. Technol.*, **191**, 155 (2005).
4. H. J. Zhang and D. Z. Wen, *Surf. Coat. Technol.*, **201**, 5720 (2007).
5. L. Miao, S. Tanemura, Y. Kondo, M. Iwata, S. Toh, and K. Kaneko, *Appl. Surf. Sci.*, **238**, 125 (2004).

6. C. Y. Jimmy, W. Ho, J. Lin, H. Yip, and P. K. Wong, *Environ. Sci. Technol.*, **37**, 2296 (2003).
7. H. Szymanowski, A. Sobczyk, M. Gazicki-Lipman, W. Jakubowski, and L. Klimek, *Surf. Coat. Technol.*, **200**, 1036 (2005).
8. H. Coleman, C. Marquis, J. Scott, S. S. Chin, and R. Amal, *Chem. Eng. J.*, **113**, 55 (2005).
9. S. Si, K. Huang, X. Wang, M. Huang, and H. Chen, *Thin Solid Films*, **422**, 205 (2002).
10. K. J. Shieh, M. Li, Y. H. Lee, S. D. Sheu, Y. T. Liu, and Y. C. Wang, *Nanomed. Nanotechnol. Biol. Med.*, **2**, 121 (2006).
11. E. Thimsen, N. Rastgar, and P. Biswas, *The Journal of Physical Chemistry C*, **112**, 4134 (2008).
12. W. A. Jacoby, D. M. Blake, R. D. Noble, and C. A. Koval, *J. Catal.*, **157**, 87 (1995).
13. T. N. Obee, *Environ. Sci. Technol.*, **30**, 3578 (1996).
14. K. Kabra, R. Chaudhary, and R. L. Sawhney, *Industrial & engineering chemistry research*, **43**, 7683 (2004).
15. C.-N. Chang, Y.-S. Ma, G.-C. Fang, A. C. Chao, M.-C. Tsai, and H.-F. Sung, *Chemosphere*, **56**, 1011 (2004).
16. R. Vinu, S. U. Akki, and G. Madras, *J. Hazard. Mater.*, **176**, 765 (2010).
17. Y. Zhang, J. W. C. Wong, P. Liu, and M. Yuan, *J. Hazard. Mater.*, **191**, 136 (2011).
18. K. Vasilev, Z. Poh, K. Kant, J. Chan, A. Michelmore, and D. Losic, *Biomaterials*, **31**, 532 (2010).
19. A. Mills, R. H. Davies, and D. Worsley, *Chem. Soc. Rev.*, **22**, 417 (1993).
20. A. Fujishima, T. N. Rao, and D. A. Tryk, *Journal of Photochemistry and Photobiology C: Photochemistry Reviews*, **1**, 1 (2000).
21. X. Li, H. Liu, L. Cheng, and H. Tong, *Environ. Sci. Technol.*, **37**, 3989 (2003).
22. A. Haarstrick, O. M. Kut, and E. Heinzle, *Environ. Sci. Technol.*, **30**, 817 (1996).
23. P. Zeman and S. Takabayashi, *Thin Solid Films*, **433**, 57 (2003).
24. M. H. Habibi, N. Talebian, and J. H. Choi, *Dyes and pigments*, **73**, 103 (2007).
25. U. Backman, A. Auvinen, and J. K. Jokiniemi, *Surf. Coat. Technol.*, **192**, 81 (2005).
26. S. Campbell, H. S. Kim, D. Gilmer, B. He, T. Ma, and W. Gladfelter, *IBM J. Res. Dev.*, **43**, 383 (1999).
27. J.-H. Kim, S. Lee, and H.-S. Im, *Appl. Surf. Sci.*, **151**, 6 (1999).
28. Z. Liu, H. Bai, and D. Sun, *Applied Catalysis B: Environmental*, **104**, 234 (2011).
29. B. H. Kim, J. H. Ahn, J. H. Jeong, Y. S. Jeon, K. O. Jeon, and K. S. Hwang, *Ceram. Int.*, **32**, 223 (2006).
30. K. Patil, S. Sathaye, Y. Khollam, S. Deshpande, N. Pawaskar, and A. Mandale, *Mater. Lett.*, **57**, 1775 (2003).
31. A. I. Kontos, A. G. Kontos, D. S. Tsoukleris, M.-C. Bernard, N. Spyrellis, and P. Falaras, *J. Mater. Process. Technol.*, **196**, 243 (2008).
32. L. Cheng, Y. Wang, S. Dai, Q. Wu, and K. Wang, *Chin. J. Mater. Res.*, **4** (1996).
33. J. Ryu, D.-S. Park, B.-D. Hahn, J.-J. Choi, W.-H. Yoon, K.-Y. Kim, and H.-S. Yun, *Applied Catalysis B: Environmental*, **83**, 1 (2008).
34. L. B. Modesto-Lopez and P. Biswas, *J. Aerosol Sci.*, **41**, 790 (2010).
35. C. Chen, E. Kelder, and J. Schoonman, *Thin Solid Films*, **342**, 35 (1999).
36. H. Yoon, J. H. Woo, Y. M. Ra, S. S. Yoon, H. Y. Kim, S. J. Ahn, J. H. Yun, J. Gwak, K. H. Yoon, and S. C. James, *Aerosol Sci. Technol.*, **45**, 1448 (2011).
37. A. Mills, G. Hill, M. Crow, and S. Hodgen, *J. Appl. Electrochem.*, **35**, 641 (2005).
38. N. R. Neti, G. R. Parmar, S. Bakardjieva, and J. Subrt, *Chem. Eng. J.*, **163**, 219 (2010).
39. T. D. Nguyen-Phan, V. H. Pham, T. V. Cuong, S. H. Hahn, E. J. Kim, J. S. Chung, S. H. Hur, and E. W. Shin, *Mater. Lett.*, **64**, 1387 (2010).
40. S. Biswas, A. Majumder, M. Hossain, T. Takahashi, Y. Kubota, and A. Fujishima, *Journal of Vacuum Science & Technology A: Vacuum, Surfaces, and Films*, **26**, 678 (2008).
41. B. A. Akgun, A. W. Wren, C. Durucan, M. R. Towler, and N. P. Mellott, *J. Sol-Gel Sci. Technol.*, 1 (2011).
42. R. A. Spurr and H. Myers, *Anal. Chem.*, **29**, 760 (1957).
43. Y. Zhang, J. Wan, and Y. Ke, *J. Hazard. Mater.*, **177**, 750 (2010).
44. F. Sayılkan, M. Asiltürk, N. Kiraz, E. Burunkaya, E. Arpaç, and H. Sayılkan, *J. Hazard. Mater.*, **162**, 1309 (2009).
45. J.-Y. Choi, K.-H. Kim, K.-C. Choy, K.-T. Oh, and K.-N. Kim, *Journal of Biomedical Materials Research Part B: Applied Biomaterials*, **80B**, 353 (2007).
46. Y. Joya, Z. Liu, and T. Wang, *ApPhB*, 1 (2011).
47. C. Srinivasan and N. Somasundaram, *Current Science*, **85**, 1431 (2003).